JACS
JOURNAL OF THE AMERICAN CHEMICAL SOCIETY
Article
pubs.acs.org/JACS

Key Mechanistic Features of Ni-Catalyzed C−H/C−O Biaryl Coupling of Azoles and Naphthalen-2-yl Pivalates

Huiying Xu,[†,‡] Kei Muto,[§] Junichiro Yamaguchi,[§] Cunyuan Zhao,[‡] Kenichiro Itami,*[,§,∥] and Djamaladdin G. Musaev*[,†]

[†]Cherry L. Emerson Center for Scientific Computation, Emory University, 1515 Dickey Drive, Atlanta, Georgia 30322, United States
[‡]School of Chemistry and Chemical Engineering, Sun Yat-Sen University, Guangzhou 510275, P. R. China
[§]Institute of Transformative Bio-Molecules (WPI-ITbM) and Graduate School of Science and [∥]JST-ERATO, Itami Molecular Nanocarbon Project, Nagoya University, Nagoya 464-8602, Japan

Supporting Information

ABSTRACT: The mechanism of the Ni-dcype-catalyzed C−H/C−O coupling of benzoxazole and naphthalen-2-yl pivalate was studied. Special attention was devoted to the base effect in the C−O oxidative addition and C−H activation steps as well as the C−H substrate effect in the C−H activation step. No base effect in the C(aryl)−O oxidative addition to Ni-dcype was found, but the nature of the base and C−H substrate plays a crucial role in the following C−H activation. In the absence of base, the azole C−H activation initiated by the C−O oxidative addition product Ni(dcype)(Naph)(PivO), **1B**, proceeds via ΔG = 34.7 kcal/mol barrier. Addition of Cs_2CO_3 base to the reaction mixture forms the Ni(dcype)(Naph)[PivOCs·$CsCO_3$], **3_Cs_clus**, cluster complex rather than undergoing $PivO^- \rightarrow CsCO_3^-$ ligand exchange. Coordination of azole to the resulting **3_Cs_clus** complex forms intermediate with a weak Cs−heteroatom(azole) bond, the existence of which increases acidity of the activated C−H bond and reduces C−H activation barrier. This conclusion from computation is consistent with experiments showing that the addition of Cs_2CO_3 to the reaction mixture of **1B** and benzoxazole increases yield of C−H/C−O coupling from 32% to 67% and makes the reaction faster by 3-fold. This emerging mechanistic knowledge was validated by further exploring base and C−H substrate effects via replacing Cs_2CO_3 with K_2CO_3 and benzoxazole (**1a**) with 1*H*-benzo[*d*]imidazole (**1b**) or quinazoline (**1c**). We proposed the modified catalytic cycle for the Ni(cod)(dcype)-catalyzed C−H/C−O coupling of benzoxazole and naphthalen-2-yl pivalate.

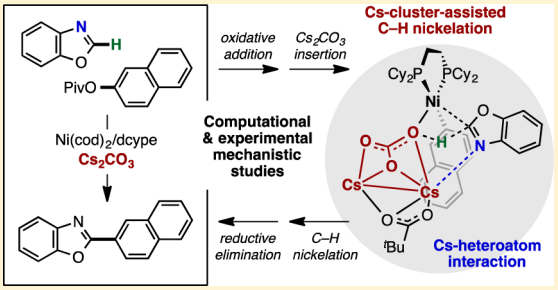

1. INTRODUCTION

Transformation of C−H bonds with a transition-metal catalyst has received significant attention in the synthetic chemistry community.[1] In recent years, site-selective C−H activation has emerged as an ideal methodology for synthesizing pharmaceutically relevant molecules, natural products, and organic π-materials. As an example, impressive progress on the direct C−H coupling methodology for making biaryls and heterobiaryls (mainly palladium-based systems) was achieved.[2] In 2012, we have shown[3] that a nickel catalyst, prepared from $Ni(cod)_2$ (cod =1,5-cyclooctadiene) and dcype (1,2-bis(dicyclohexylphosphino)ethane), activates both C−H bond of 1,3-azoles and C−O bond of phenol derivatives and facilitates heterobiaryl formation (Scheme 1). More recently,[4] we have reported a number of experimental results that are in line with our initial mechanistic blueprint for the C−H/C−O biaryl coupling, consisting of (1) C(aryl)−O bond oxidative addition of the phenol derivative (Ar−OR) to Ni(0) leading to Ar−Ni−OR intermediate, (2) C−H activation/nickelation of azole (Az−H) by the resulting Ar−Ni−OR intermediate to form an Ar−Ni−Az intermediate, and (3) Ar−Ar reductive elimination from the Ar−Ni−Az intermediate to regenerate Ni(0) catalyst (Scheme 1).

However, in order to develop next-generation nickel catalysts with broader substrate scope, it is critically important to gain insight into the mechanism and controlling factors of the C−H/C−O coupling reaction by means of a joint experimental and computational approach.

After our initial experimental report on the Ni-dcype-catalyzed C−H/C−O coupling of azoles and phenol derivatives,[3] several studies on the mechanism of this class of reaction were reported.[5] Just recently, Fu and co-workers have computationally shown that the steric hindrance of the C−O electrophile suppresses the decarbonylative C−H coupling.[6] Previously, a similar finding was experimentally reported for a closely related catalytic system.[7] In addition, Fu and co-workers have emphasized importance of the PhO-to-K_2PO_4 ligand exchange, upon addition of K_3PO_4 base to reaction mixture, in the Ni-dcype-catalyzed coupling reaction between benzoxazole and phenyl pivalate.

Received: July 14, 2014
Published: September 26, 2014

dx.doi.org/10.1021/ja5071174 | J. Am. Chem. Soc. 2014, 136, 14834−14844

Scheme 1. C−H/C−O Biaryl Coupling by Ni-dcype Catalyst

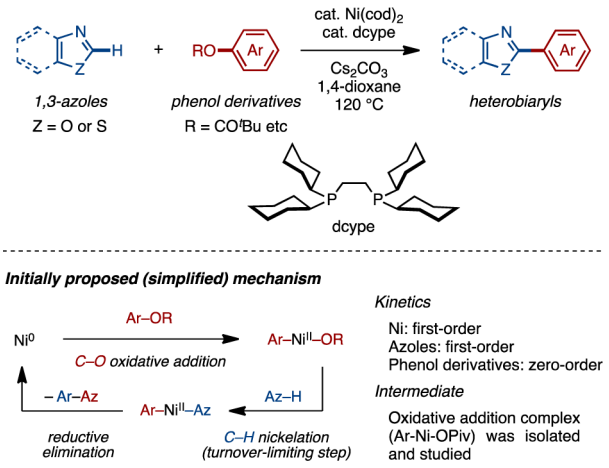

In spite of these and several other advances, still various aspects of this chemically important reaction, especially those related to the nature of C−H substrate and role of base in the C−H/C−O coupling, remain to be answered. Although the ultimate purpose of our joint computational and experimental activity is to elucidate the factors governing each elementary reaction involved in the Ni-dcype-catalyzed C−H/C−O biaryl coupling (Scheme 1), in this paper we intend to elucidate in particular (1) the base effect in the naphthalen-2-yl pivalate (NaphOPiv) C−O oxidative addition and C−H activation/nickelation steps and (2) the C−H substrate effect in the stoichiometric reaction of the oxidative addition product Ni(Naph)(OPiv)(dcype) (**1B**) with various azoles (Scheme 2).

Scheme 2. Schematic Presentation of the Studied (1) NaphOPiv C−O Oxidative Addition to Ni(dcype)(cod) and (2) Stoichiometric Reaction of the Oxidative Addition Product 1B with Various Azoles

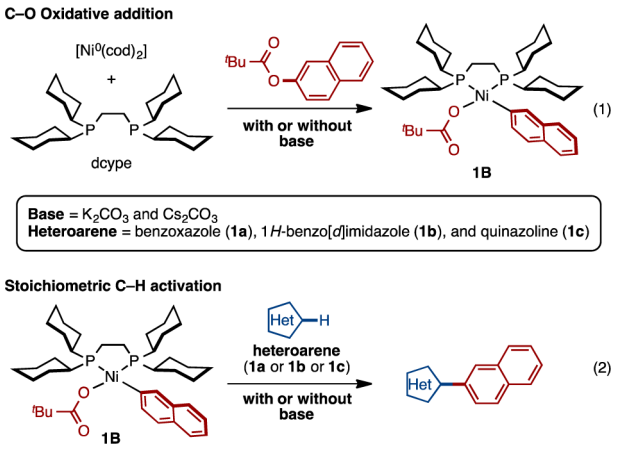

One should emphasize that we have previously isolated and characterized the C(aryl)−O oxidative addition product Ni(Naph)(OPiv)(dcype) upon reaction of nickel catalyst [prepared from $Ni(cod)_2$ and dcype ligand] with NaphOPiv in toluene at 100 °C.

2. COMPUTATIONAL DETAILS

Calculations were performed by Gaussian 09 quantum chemical package.[8] The geometries of all reported reactants, intermediates, transition states, and products were optimized without symmetry constraints in 1,4-dioxane solvent (ε = 2.21) at the M06L level of density functional theory[9] in conjunction with the Lanl2dz basis set and corresponding Hay−Wadt effective core potential (ECP) for Ni and Cs.[10] Standard 6-31G(d) basis sets were used for all other atoms. Below, this approach will be called as M06L/{Lanl2dz + [6-31G(d)]} or M06L/BS1. Solvent effects were estimated by using the PCM solvation method.[11] In order to incorporate disperse interactions into calculations we also performed geometry optimization and energy calculations of selected important intermediates and transition states at the M06/BS1 level of theory.[12] These calculations have shown that the M06L/BS1 and M06/BS1 optimized geometries are very close, while relative energies can vary by a few kcal/mol (see the Supporting Information (SI)). The nature of each stationary point was characterized by performing normal-mode analysis. Relative free energies and enthalpies of all reported structures were calculated under standard conditions (1 atm and 298.15 K). Since the associated experiments were performed at 100 °C (see Scheme 2), the important energy barriers [i.e., C(aryl)−O oxidative addition and benzoxazole C−H bond activation] were also recalculated at 373.15 K. Briefly, it is found that increasing the temperature from 298.15 to 373.15 K only slightly increases energy barriers and does not affect the reported conclusions and reactivity trends. Therefore, below, in sake of consistency, we discuss the M06/BS1 calculated free energies (i.e., ΔG values) at 298.15 K unless otherwise specified. In the presented figures and tables, we give both relative Gibbs free energies and enthalpies (in kcal/mol) as $\Delta G/\Delta H$. Cartesian coordinates and total energies of all reported structures are given in the SI.

In order to evaluate the used M06L/BS1 and M06/BS1 approaches we investigated the geometry of the $Ni(dcype)(CO)_2$ complex, which was previously isolated experimentally and characterized by X-ray technique.[7] Comparison of the calculated geometry parameters of this molecule with their X-ray values shows an excellent agreement between the calculated and experimental geometries of $Ni(dcype)(CO)_2$ (see SI).

3. RESULTS AND DISCUSSIONS

As mentioned above, the purpose of this paper is to elucidate the base effect in the C−O oxidative addition step, as well as the C−H substrate and base effects in the reaction of the oxidative addition product **1B** and substrate, i.e. ,C−H activation/nickelation and reductive elimination steps (Scheme 2). However, first we will briefly comment on a few important issues related to the generation of the active catalyst because of their importance to the consequent discussions.

Consistent with available experiment,[13] our calculations (see SI) show that active catalyst formation, i.e., the reaction $Ni(cod)_2$ + dcype → Ni(cod)(dcype) + cod is 12.5 kcal/mol exergonic. Substitution of cod by NaphOPiv in Ni(cod)(dcype) is expected to be the next step of the reaction, and this step may proceed differently in *absence* and *presence* of base in the reaction mixture.

In the absence of base, the cod → NaphOPiv substitution in Ni(cod)(dcype) leads to Ni(dcype)(NaphOPiv) intermediate which has numerous isomers, among which isomers **A**, **B**, and **C** (see SI) [where the aryl pivalate ligand is coordinated to nickel through the C=O double bond of its carboxylate fragment, the C=C double bond of its arene ring and carbonyl−O, and the C=C double bond of its arene ring and μ_2-O of its carboxylate group, respectively] are lower in energy. Although these isomers could transform to each other, they should be considered as prereaction complexes in the C(acyl)−O and C(aryl)−O oxidative addition reactions.

Factors affecting selectivity of the C(aryl)−O and C(acyl)−O bond activation have been subject of several recent investigations.[5a,6,14] Our calculations mostly agree with previous studies but also provide slightly different results (see SI). First, we find

dx.doi.org/10.1021/ja5071174 | J. Am. Chem. Soc. 2014, 136, 14834−14844

that the C(acyl)−O bond cleavage, proceeding via a *three-centered* transition state, requires a 26.7 kcal/mol energy barrier and is 11.4 kcal/mol endergonic (calculated relative to the reactants [Ni(cod)(dcype) + NaphOPiv]. Second, the C(aryl)−O oxidative addition, occurring via the *five-centered* transition state **TS1B** (see Figure 1), requires a slightly higher (29.1 kcal/mol)

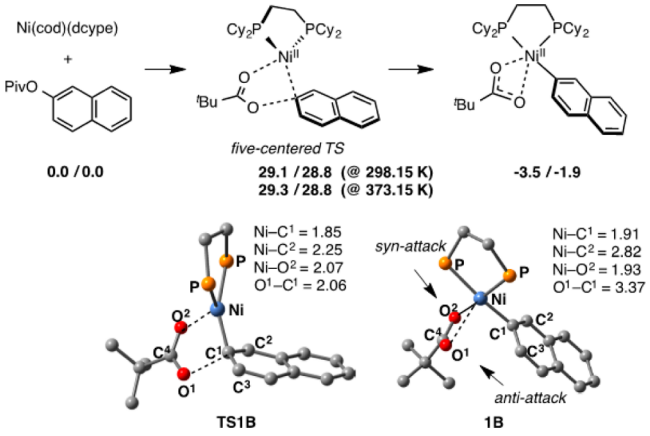

Figure 1. Important geometry parameters (in Å) and relative energies [in kcal/mol, relative to reactants Ni(cod)(dcype) plus NaphOPiv] of the lowest C(aryl)−O oxidative addition five-centered transition state and corresponding oxidative addition product **1B** (cyclohexyl groups and hydrogen atoms are omitted for clarity).

energy barrier and leads to product **1B**. However, the C(aryl)−O oxidative addition is found to be 3.5 kcal/mol exergonic. Based on these findings, we predict the C−O oxidative addition product of the reaction of Ni(cod)(dcype) with NaphOPiv to be the Ni(Naph)(OPiv)(dcype), **1B**, complex associated with the C(aryl)−O oxidative addition. This prediction is consistent with our recent experiments showing that the reaction of Ni(cod)(dcype) with NaphOPiv leads to isolable and stable Ni(Naph)(OPiv)(dcype) product.[4] One should note that increasing temperature from 298.15 to 373.15 K increases the energy barrier associated with the C(aryl)−O oxidative addition transition state **TS1B** from 29.1 to 29.3 kcal/mol. One should also mention that the calculated geometry parameters (Figure 1) of oxidative addition product **1B** are consistent with their experimental values (see SI).[4]

In the presence of base, the C−O oxidative addition to Ni(cod)(dcype) is expected to be very complicated and can be affected by numerous factors such as (but not limited to) the chemical nature of base, its aggregation state (i.e., availability of the base molecule), and concentration of the base molecule in the reaction mixture. Our limited computational data (see SI) indicate that the C(aryl)−O oxidative addition of NaphOPiv to Ni(cod)(dcype) is a facile process in the presence of both Cs_2CO_3 and K_2CO_3. However, these studies have also indicated that this oxidative addition process in the presence of base requires more comprehensive approaches and cannot be conclusively solved exclusively by computation.

Therefore, we turned to experiments to investigate the influence of base on the C−O oxidative addition to Ni(cod)(dcype). We monitored the C−O oxidative addition reaction of NaphOPiv in the presence of Cs_2CO_3 or K_2CO_3 by ^{31}P NMR spectroscopy (Figure 2). In comparison with the reaction in the absence of base, the use of neither Cs_2CO_3 nor K_2CO_3 showed significant effect on the oxidative addition. Both reactions completed in 8 h. In the course of these reactions, only ^{31}P

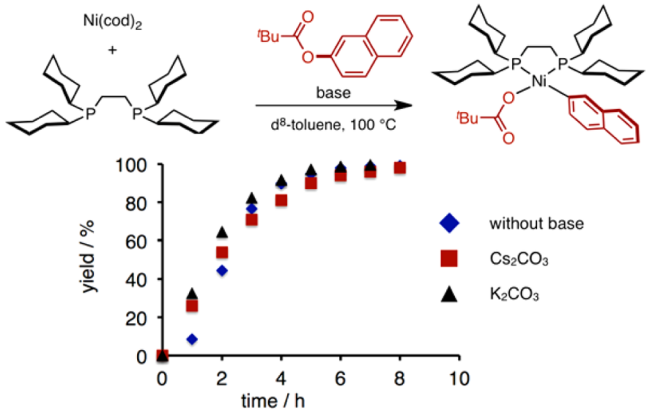

Figure 2. Monitoring the C−O oxidative addition of NaphOPiv to Ni(cod)(dcype) in the presence (dark, K_2CO_3 and brown, Cs_2CO_3) and absence (blue) of base.

NMR peaks, derived from product Ni(Naph)(OPiv)(dcype) and reactant Ni(cod)(dcype) complexes, were observed. These results indicate that the C−O oxidative addition is not affected by the Cs_2CO_3 and K_2CO_3.

3.1. C−H Activation/Nickelation. Previously, we reported[4] that the stoichiometric reaction of Ni(Naph)(OPiv)(dcype) (**1B**) and benzoxazole gave the coupling product, but the reaction yield increases from 32% to 67% upon addition of Cs_2CO_3 to the reaction mixture (Scheme 2). Furthermore, the performed kinetic study on the stoichiometric reaction of **1B** with benzoxazole in the presence and absence of bases (see SIs for more details) shows that the reaction in the presence of Cs_2CO_3 is 3-fold faster than the reaction without bases (see Figure 3). These findings of our previous[4] and current

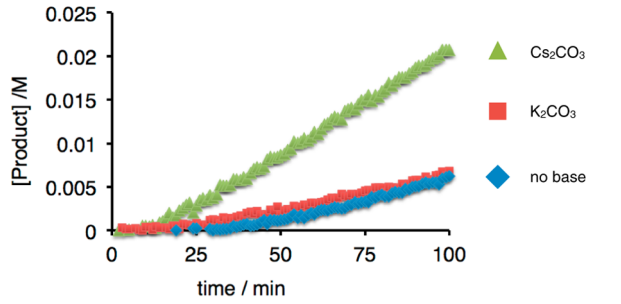

Figure 3. Monitoring the kinetics of the stoichiometric reaction of **1B** with benzoxazole in the presence (K_2CO_3, brown, and Cs_2CO_3, green) and absence (blue) of base.

experiments indicate the intervention of base in the mechanism of the C−H activation/nickelation step. In order to elucidate the mechanism of the C−H activation/nickelation as well as the role of the base in this process, we investigated two distinct reactions of **1B** with benzoxazole. One of them does not involve base, while another one includes Cs_2CO_3 in the reaction mixture.

3.1.1. C−H Activation/Nickelation in the Absence of Base. The C−H activation/nickelation is expected to be initiated by coordination of benzoxazole to the C(aryl)−O oxidative addition product **1B**. Due to the unsymmetrical nature of naphthalenyl group, benzoxazole can attack to **1B** from either *syn* or *anti* directions to the bending side of naphthalenyl ligand (Figure 1). In general, calculations show that both pathways proceed via the same mechanisms, while the *anti*-attack requires

dx.doi.org/10.1021/ja5071174 | J. Am. Chem. Soc. 2014, 136, 14834−14844

slightly higher C−H activation barrier (see SI). Therefore, below we only report details of the *syn*-attack of benzoxazole to **1B**.

Coordination of benzoxazole to **1B** results in intermediate **2a**, which lies 15.2 kcal/mol higher in free energy than dissociation limit of **1B** + azole (see Figure 4). The following azole C−H activation occurs via traditional concerted metalation/deprotonation (CMD)[15] transition state **TS2a**. As seen in Figure 4, in **TS2a**, one of oxygen atoms (O^1) of pivalate is

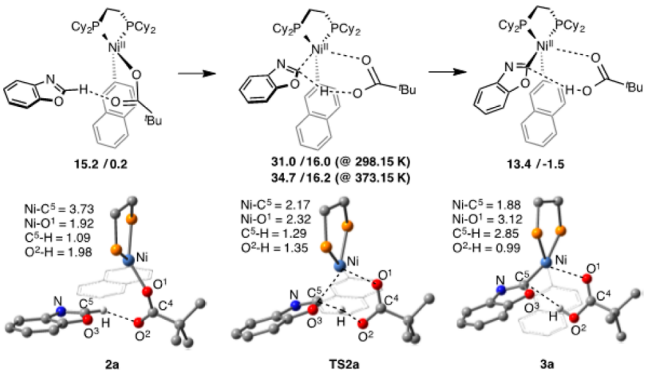

Figure 4. Important geometry parameters (in Å) and relative energies (in kcal/mol, relative to the reactants **1B** + benzoxazole) of the intermediate **2a**, C−H nickelation transition state **TS2a**, and C−H nickelation product **3a** (cyclohexyl groups and selected hydrogen atoms are omitted for clarity).

weakly coordinated to the nickel center, while another one (O^2) is engaged in proton abstraction from the C^5-center. The C^5 atom of azole also interacts with the nickel center. Important geometry parameters of transition state **TS2a**, i.e., the Ni−C^5, Ni−O^1, C^5−H, and O^2−H distances are 2.17, 2.32, 1.29, and 1.35 Å, respectively.

The energy barrier required at the transition state **TS2a** is 31.0 kcal/mol. The formation of product **3a** is endergonic by 13.4 kcal/mol. In an aim to find an energetically less demanding pathway we have also investigated C−H activation via the *arm-off* mechanism (i.e., via formation of coordinatively unsaturated nickel complex by cleaving one of the two Ni−P bonds), which has been extensively discussed in literature.[6,16] However, we found that the *arm-off* mechanism requires an even larger energy barrier of 37.7 kcal/mol (see SI) and, therefore, is excluded from further discussion.

From the resulting intermediate **3a**, reaction may proceed either via the PivOH dissociation (i.e., formation of intermediate **4a**, see Figure 5) and then C−C reductive elimination or via the direct C−C reductive elimination and then PivOH dissociation pathways. Between these two pathways, we found the pathway proceeding via the PivOH dissociation followed by C−C reductive elimination to be energetically more feasible. The first step of this pathway, i.e., PivOH dissociation (**3a** → **4a**), is exergonic, 4.5 kcal/mol, while its second step, i.e., C−C reductive elimination, requires a small energy barrier 9.1 kcal/mol at the transition state **TS3a** (see Figure 5).

The calculated small energy barrier for the C−C reductive elimination is consistent with previous reports on the facile $C(sp^3)$−$C(sp^3)$, $C(sp^3)$−$C(sp^2)$, and $C(sp^2)$−$C(sp^2)$ coupling in Pd(II) and Ni(II) systems.[17,18] The formation of biaryl complex **5a** is found to be 16.0 kcal/mol exergonic, relative to the reactants **1B** plus benzoxazole.

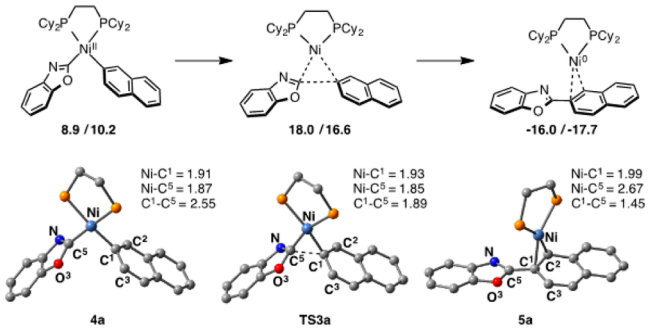

Figure 5. Important geometry parameters (in Å) and relative energies (in kcal/mol, relative to the reactants **1B** + benzoxazole) of the intermediate **4a**, reductive elimination transition state **TS3a**, and C−C coupling complex **5a** (cyclohexyl groups and hydrogen atoms are omitted for clarity).

As seen from the overall potential energy surface (PES) of the reaction in Figure 6, the C−C reductive elimination proceeds via a much smaller energy barrier than that required for the reverse (i.e., the C−H formation) reaction **4a** → **TS2a** → **2a**. Therefore, the reaction of **1B** and benzoxazole, in the absence of base, will require a total of 31.0 kcal/mol C−H nickelation/activation barrier at the transition state **TS2a**. Increasing the temperature from 298.15 to 373.15 K increases this energy barrier from 31.0 to 34.7 kcal/mol, which is 5.4 kcal/mol larger than 29.3 kcal/mol barrier required for the C(aryl)−O oxidative addition to Ni(cod)(dcype). This conclusion is consistent with the experimentally reported high reaction temperature (100−120 °C) and rate-determining C−H activation step.

3.1.2. Cs_2CO_3-Mediated C−H Activation/Nickelation. Thus, in the absence of base, the C−H activation/nickelation reaction of Ni(Naph)(OPiv)(dcype) (**1B**) and benzoxazole requires 34.7 kcal/mol barrier (31.0 kcal/mol at 298.15 K) at the CMD transition state **TS2a**. However, as already mentioned, our experiments show that the addition of Cs_2CO_3 to the reaction mixture increases yield of the C−H/C−O biaryl coupling from 32% to 67% (Scheme 2)[4] and makes the reaction faster by a factor of 3 (Figure 3). Therefore, in this section we explore the roles of Cs_2CO_3 in the stoichiometric reaction of **1B** and benzoxazole.

We should emphasize that the importance of base (carbonates, such as Cs_2CO_3, K_2CO_3, etc.) and cocatalysts (carboxylic acids, such as AcOH, CsOPiv, KOPiv, etc.) is widely recognized in the transition-metal-catalyzed $C(sp^2)$−H and $C(sp^3)$−H bond functionalization reactions.[19] For example, it was shown that addition of carboxylate acid and base is absolutely necessary for success of the Pd-catalyzed direct arylation of arenes and alkanes.[15a,20] It was suggested that, in these reactions, the carboxylic acids act *exclusively* as a proton shuttle in the concerted metalation/deprotonation (CMD) transition state, while the stoichiometric carbonate or phosphate plays the role of either proton scavenger from the acetic acid or aids in the removal of acetic acid from the reaction mixture[21] at the subsequent stage of the reaction to make the deprotonation process irreversible.[22] Unfortunately, this mechanistic picture does not explain the observed increase yield of the reaction **1B** with benzoxazole upon addition of Cs_2CO_3 to the reaction mixture. Furthermore, previously reported studies failed to explain roles of the countercation in the C−H activation/metalation, partly because most of the existing mechanistic studies either completely ignored countercation in the modeling[23] or reduced

dx.doi.org/10.1021/ja5071174 | J. Am. Chem. Soc. 2014, 136, 14834−14844

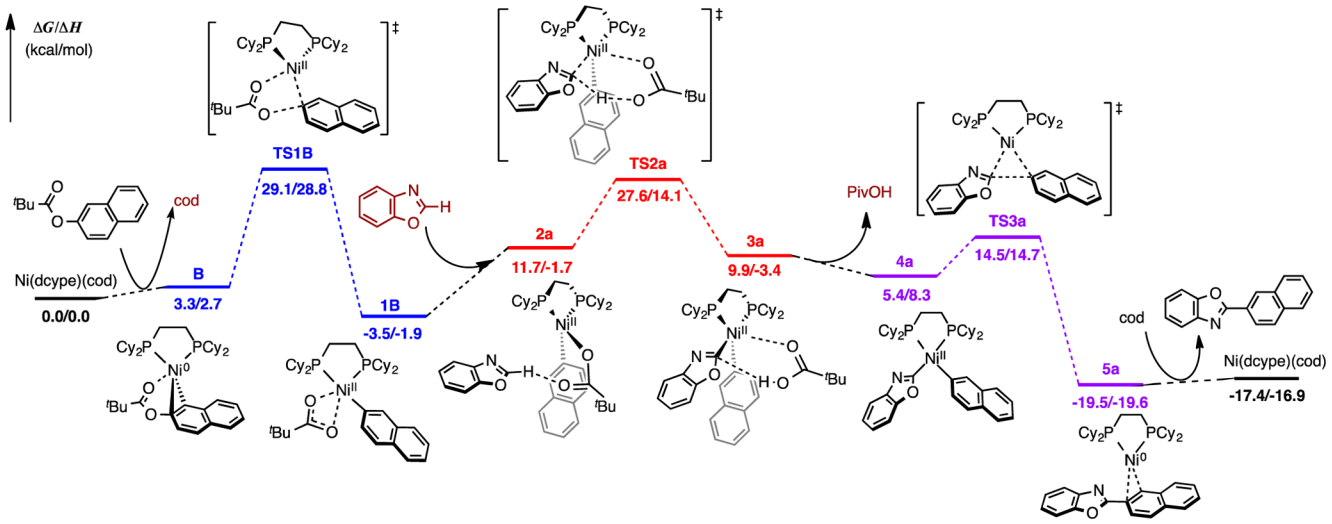

Figure 6. Overall PES of the Ni(dcype)(cod)-catalyzed C−H/C−O biaryl coupling reaction without base.

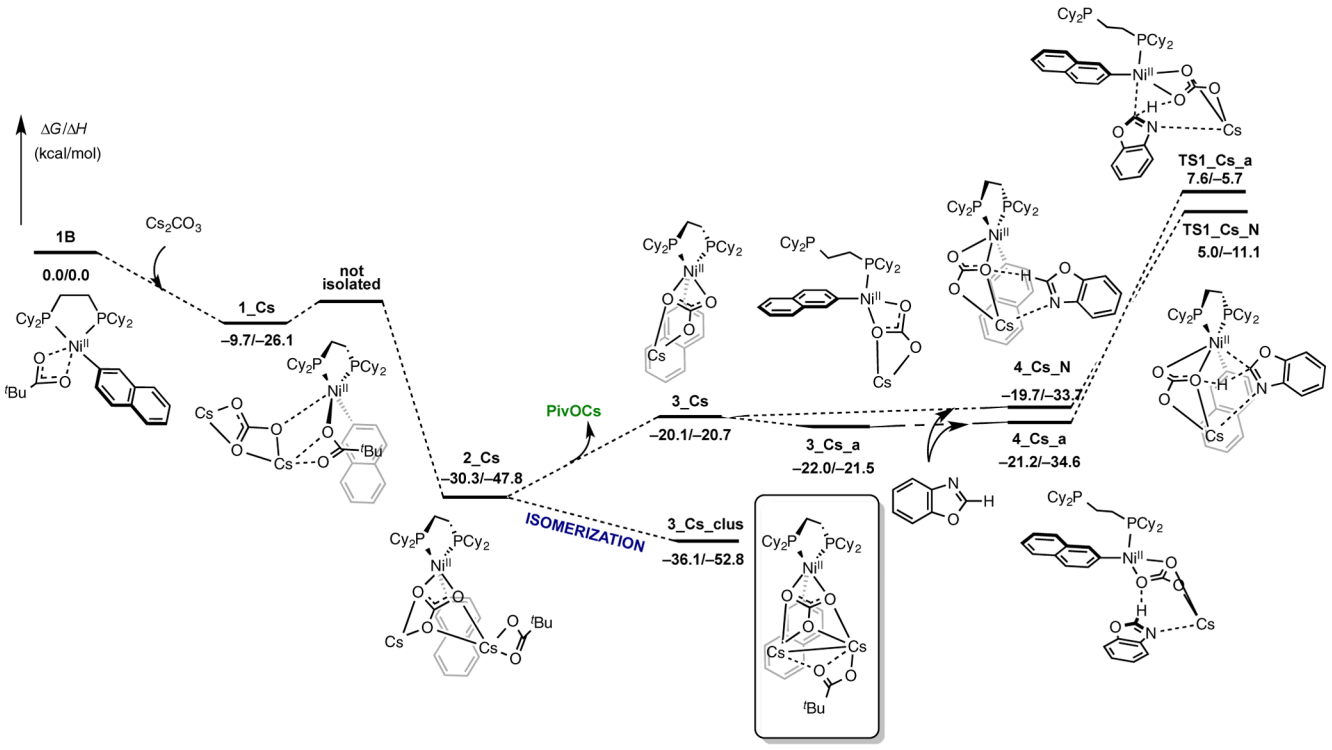

Figure 7. Potential energy profile of the reaction **1B** + Cs_2CO_3 → **2_Cs** as well as following Ni(dcype)(Naph)[PivOCs·$CsCO_3$] cluster complex **3_Cs_clus** formation and alternative $PivO^-$ to $CsCO_3^-$ ligand exchange pathways.

the role of additive (carboxylate acids, percarbonates, phosphates etc.) to simple ligand (anion) exchange.[6]

The present study includes real-sized (used in the experiments) systems as well as both counter-cations and corresponding anions into the calculations. The addition of Cs_2CO_3 to **1B** is found to be 9.7 kcal/mol exergonic. It leads to the formation of **1_Cs** intermediate (see Figure 7), which is kinetically less stable and transforms to the thermodynamically more favorable intermediate **2_Cs**: the reaction **1B** + Cs_2CO_3 → **2_Cs** is 30.3 kcal/mol exergonic. From the resultant complex **2_Cs**, the reaction may proceed via two different pathways. The first begins with the elimination of PivOCs to form complex **3_Cs** and a $CsCO_3$ anion, i.e., so-called $PivO^-$ to $CsCO_3^-$ ligand exchange pathway. This process requires 10.2 kcal/mol free energy. Furthermore, the following C−H activation from the resulting complex **3_Cs** with either bidentately or monodentately (*i.e. arm-off* path) coordinated dcype ligand requires an additional high activation barrier: the total energy required for the C−H activation/nickelation calculated from **2_Cs** for bidentately and monodentately coordinated dcype ligand is found to be 35.3 and 37.9 kcal/mol, respectively. One should note that similar results on the ligand exchange, i.e., reaction Ni(dcype)(Ph)(RCOO) + K_3PO_4 → Ni(dcype)(Ph)(K_2PO_4) + RCOOK, and base-assisted benzoxazole C−H bond activation (where R = ^{t}Bu and thiophene, C_4SH_3) were reported by Fu and co-workers.[6]

Strikingly, our calculations show that complex **2_Cs** will rather easily (with several energetically less demanding transition

dx.doi.org/10.1021/ja5071174 | J. Am. Chem. Soc. 2014, 136, 14834−14844

states and shallow minima) isomerize to the thermodynamically more stable cluster complex **3_Cs_clus**. The **2_Cs**-to-**3_Cs_clus** transformation is found to be 5.8 kcal/mol exergonic, while overall reaction **1B** + Cs_2CO_3 → **3_Cs_clus** is highly exergonic (36.1 kcal/mol). In the resultant cluster complex **3_Cs_clus** (see Figures 7 and 8), the [PivOCs·$CsCO_3$]$^-$ cluster anion is strongly bound to the Ni-center. Based on these findings, we predict the cluster complex **3_Cs_clus** to be the thermodynamically most favorable prereaction complex in the Cs_2CO_3, **1B**, and substrate reaction mixture.

At the next stage, the resultant cluster complex **3_Cs_clus** coordinates substrate and acts as an active catalyst for the benzoxazole C−H activation. In general, the benzoxazole molecule may coordinate to **3_Cs_clus** from two distinct directions (see Figure 8): *syn*, from the side to where the

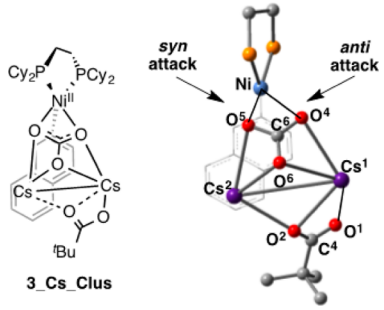

Figure 8. *Syn* and *anti* approaches of benzoxazole to the complex **3_Cs_clus**.

naphthalenyl ligand is leaning, (i.e., from the side where Cs^2 and O^5 centers are located), and *anti* (i.e., from the side where Cs^1 and O^4 centers are located). Since the substrate C−H activation via the *syn*-attack pathway is found to require slightly larger energy barrier than that for the *anti*-attack (see SI), below we only discuss mechanistic details of the *anti*-attack of benzoxazole to **3_Cs_clus**.

Anti-attack of benzoxazole to **3_Cs_clus** produces (benzoxazole)-**3_Cs_clus** complex, which may have two isomers called as **4_Cs_clus_O** and **4_Cs_clus_N** species. These isomers differ in having Cs−O(azole) and Cs−N(azole) weak bonds, respectively. As seen in Figure 9, the calculated Cs^1−O(azole) and Cs^1−N(azole) bond distances in these complexes are 3.22 and 3.22 Å, respectively. The value of the Cs^1−O(azole) bond distance in **4_Cs_clus_O** is longer than 3.07 Å reported for $Cs(H_2O)_n^+$ and 3.00 Å of sum of the covalent radii of cesium and oxygen atoms.[24] The value of the Cs^1−N(azole) bond distance in **4_Cs_clus_N** is in good agreement with those reported for monocesium compounds $[Cs(LH_3)(py)]_n$ (L = calix[4]arene) [3.098(16) Å], $[Cs\{([Me_3Si]_2C)P(C_6H_4CH_2NMe_2)_2\}(toluene)]_n$ [3.2758(19) and 3.1039(17) Å], the amide-bridged dimeric complex $[\{Cs(\mu\text{-TMP})(TMEDA)\}_2]$ [Cs−N = 3.198(2) Å, TMP = 2,2,6,6-tetramethylpiperidide],[25] and the sum of covalent radii of cesium and nitrogen atoms (3.03 Å).

Since the stoichiometric reaction **1B** + Cs_2CO_3 + benzoxazole was conducted in 1,4-dioxane and toluene solutions, and previously[26] it was shown that 1,4-dioxane molecules could solvate Cs cation by forming Cs−O(dioxane) bonds, here we elucidated the impact of 1,4-dioxane coordination to the reported Cs−N(azole) interaction in intermediate **4_Cs_clus_N**.

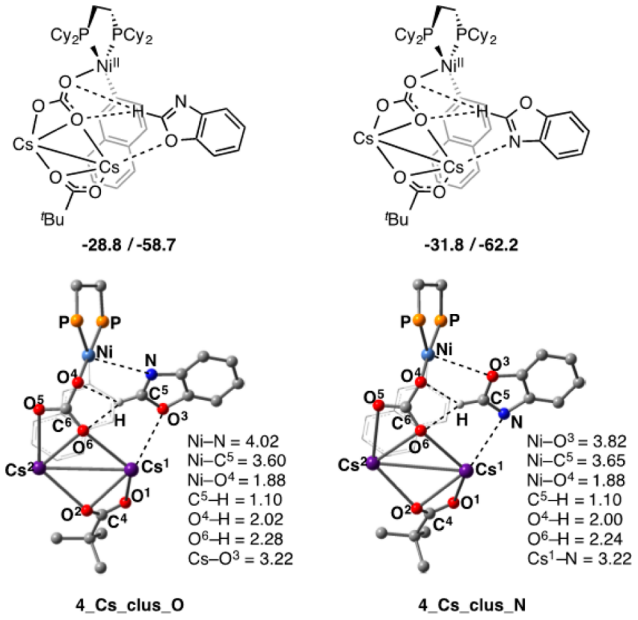

Figure 9. Important geometry parameters (in Å) and relative energies [in kcal/mol, relative to reactants **1B** + Cs_2CO_3 + benzoxazole] of the intermediates **4_Cs_clus_O** and **4_Cs_clus_N** with Cs−O(azole) and Cs−N(azole) weak bonds, respectively (cyclohexyl groups and selected hydrogen atoms are omitted for clarity).

For this reason, we included several 1,4-dioxane molecules into the calculations (see Figure S17 of SI for more details). These calculations show that azole molecule interacts with **3_Cs_clus** intermediate by 8.0 kcal/mol stronger than 1,4-dioxane does, and the solvation of Cs cation by 1,4-dioxane has no impact on the above-reported Cs−N(azole) interaction. In other words, these calculation confirmed the existence of Cs−N(azole) [or Cs−O(azole)] interaction even in 1,4-dioxane solution. We envision that the existing Cs−N(azole) and Cs−O(azole) interactions may play a crucial *directing role* in the C−H nickelation. Furthermore, the existence of these interactions is expected to increase acidity of the C−H bond of coordinated benzoxazole and thus lower the CMD activation barrier. A similar effect was reported by Gorelsky in the study of Pd(II)-catalyzed direct arylation of azoles by Cu(I) coordination.[27]

Since complex **4_Cs_clus_N** is 3.0 kcal/mol more stable than **4_Cs_clus_O**, and the C−H activation reaction initiated from both complexes proceeds via the same type of intermediates and transition states (see SI), below we briefly discuss the mechanism of **4_Cs_clus_N** promoted C−H activation reaction. As shown in Figure 10, the C−H activation barrier at the transition state **TS1_Cs_clus_N** is 27.3 kcal/mol (calculated relative to the cluster complex **3_Cs_clus** + benzoxazole, at 298.15 K), i.e., by 3.7 kcal/mol less than rate-determining barrier of 31.0 kcal/mol reported for the reaction of **1B** with benzoxazole in the absence of base. Increasing the temperature from 298.15 to 373.15 K raises this energy barrier from 27.3 to 31.1 kcal/mol, which is 1.8 kcal/mol larger than 29.3 kcal/mol energy barrier required for the C(aryl)−O oxidative addition to Ni(cod)(dcype). In other words, the C−H activation step remains a rate-determining one even upon addition of Cs_2CO_3 to reaction mixture.

Thus, addition of Cs_2CO_3 to the reaction mixture of **1B** and benzoxazole, at first, produces the cluster complex **3_Cs_clus**: overall reaction of **1B** + Cs_2CO_3 → **3_Cs_clus** is 36.1 kcal/mol

dx.doi.org/10.1021/ja5071174 | J. Am. Chem. Soc. 2014, 136, 14834−14844

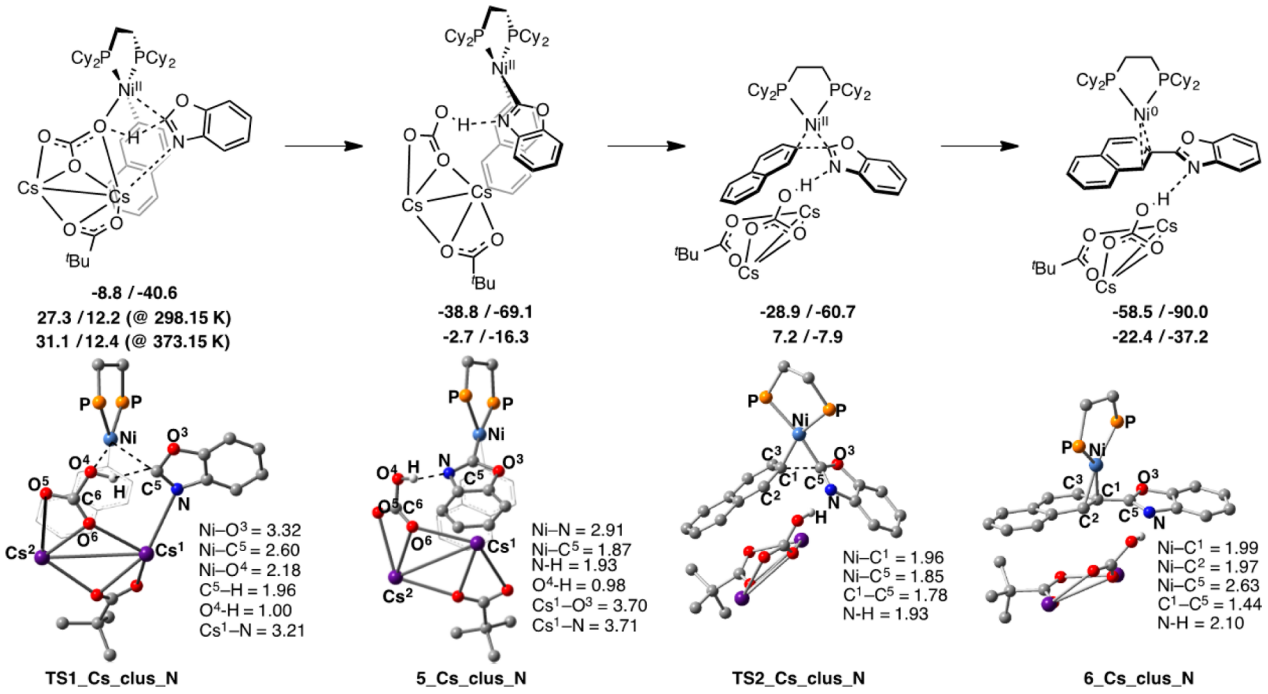

Figure 10. Important geometry parameters (in Å) and relative energies [in kcal/mol, numbers given in first line are relative to reactants **1B** + Cs_2CO_3 + benzoxazole, while those given in second line are relative to **3_Cs_clus** + benzoxazole] of transition states and products of the C−H activation [**TS1_Cs_clus_N** and **5_Cs_clus_N**] and C−C reductive elimination [**TS2_Cs_clus_N** and **6_Cs_clus_N**] steps of the reaction **1B** + Cs_2CO_3 + benzoxazole (cyclohexyl groups and selected hydrogen atoms are omitted for clarity).

exergonic (see Figure 7). The resultant complex **3_Cs_clus** coordinates the benzoxazole molecule and forms an intermediate with the Cs−heteroatom(azole) interaction (see Figure 9) that increases acidity of the activated C−H bond and lowers the C−H activation barrier. The existence of the Cs-heteroatom-(azole) interaction in pre-reaction complex (**4_Cs_clus_O** or **4_Cs_clus_N**) is predicted to be only one of the factors that reduce the rate-limiting C−H activation barrier. In general, this finding of computation is in good agreement with our experiments showing that addition of Cs_2CO_3 to the reaction mixture **1B** and benzoxazole increases the reaction yield from 32% to 67% (Scheme 2)[4] and makes the reaction faster by 3-fold (Figure 3).

Comparison of the C−H activation transition states **TS2a** and **TS1_Cs_clus_N** shows that the addition of Cs_2CO_3 to **1B** also changes the nature of the C−H activation transition state from being the six-membered CMD transition state (**TS2a**) to the four-membered σ-bond metathesis transition state where the μ_2-O (that links Ni with PivOCs·$CsCO_3$ cluster) center acts as a proton acceptor.

Overcoming the highly asynchronous σ-bond metathesis transition state **TS1_Cs_clus_N** leads to the biaryl intermediate **5_Cs_clus_N** that lies 2.7 kcal/mol lower in energy than reactants **3_Cs_clus** + benzoxazole. The C−C reductive elimination from the resulted intermediate **5_Cs_clus_N** occurs with a relatively small, 9.9 kcal/mol, energy barrier (see Figure 10) in the transition state **TS2_Cs_clus_N**. Overall reactions **1B** + Cs_2CO_3 + benzoxazole → **6_Cs_clus_N** and **3_Cs_clus** + benzoxazole → **6_Cs_clus_N** are found to be 58.5 and 22.4 kcal/mol exergonic, respectively.[28]

To summarize, the presented calculations, for the first time in the literature to our best knowledge, show that (1) the addition of Cs_2CO_3 to reaction mixture of Ni(dcype)(Naph)(OPiv) (**1B**) and benzoxazole leads to formation of the thermodynamically stable Ni(dcype)(Naph)[PivOCs·$CsCO_3$] cluster complex **3_Cs_clus** rather than the $PivO^-$ → $CsCO_3^-$ ligand exchange; (2) the coordination of benzoxazole to the cluster complex **3_Cs_clus** forms intermediates **4_Cs_clus_O** or **4_Cs_clus_N** with Cs−O(azole) and Cs−N(azole) interactions, respectively. The existence of the Cs-heteroatom(azole) interaction is predicted to be one of the factors facilitating the C−H activation in the presence of base and, consequently, increasing the reaction yield; and (3) the formation of the cluster complex **3_Cs_clus** changes the nature of the C−H activation transition states from being the six-membered CMD transition state (**TS2a**), in the no base case, to the four-membered σ-bond metathesis transition state (**TS1_Cs_clus_N**) where the μ_2-O (that links Ni with PivOCs·$CsCO_3$ cluster) center acts as a proton acceptor.

Combination of our previous experimental data[4] and aforementioned computational findings enables us to propose the modified catalytic cycle for the Ni(cod)(dcype)-catalyzed C−H/C−O biaryl coupling of benzoxazole and NaphOPiv. Now, we predict that this reaction involves the: (1) active catalyst generation and Ni(dcype)(NaphOPiv) intermediate formation, (2) C(aryl)−O oxidative addition via the five-centered transition state leading to the Ni(dcype)(Naph)(OPiv) intermediate, (3) Cs_2CO_3 coordination and the Ni(dcype)(Naph)-[PivOCs·$CsCO_3$] cluster complex formation, (4) C−H activation/nickelation by the Cs-clustered nickel complex via the σ-bond metathesis transition state, and (5) C−C reductive elimination and catalyst regeneration (see Scheme 3). One should note that understanding the roles of base in the catalyst activation and regeneration steps still requires more comprehensive investigations, which are in progress in our groups.

3.2. Proof of Concept. In order to validate above presented mechanistic details of the stoichiometric reaction of the naphthalen-2-yl pivalate C−O oxidative addition product Ni(Naph)(OPiv)(dcype) (**1B**) and C−H substrate (the C−H

dx.doi.org/10.1021/ja5071174 | J. Am. Chem. Soc. 2014, 136, 14834−14844

Scheme 3. Modified Catalytic Cycle of the Ni(cod)(dcype)-Catalyzed and [PivOCs·$CsCO_3$]-Mediated C−H/C−O Biaryl Coupling between Benzoxazole and NaphOPiv

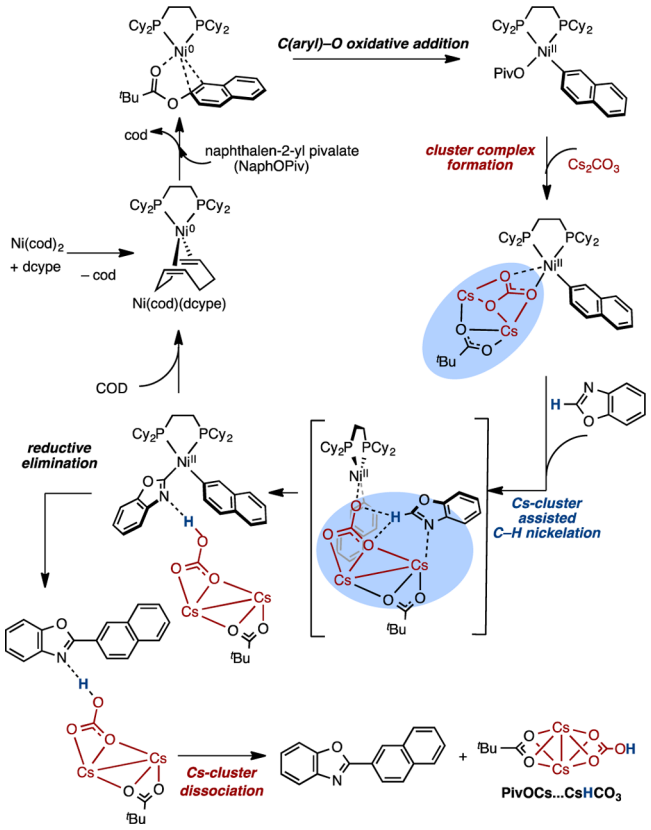

activation/nickelation and reductive elimination steps), we have extended our joint experimental and computational study to K_2CO_3 (instead of Cs_2CO_3, i.e., Cs → K replacement), benzimidazoles (instead of benzoxazole, i.e., O → N replacement) and quinazoline (instead of five-membered arene, i.e., five-membered → six-membered arene replacement).

3.2.1. K_2CO_3 vs Cs_2CO_3 in C−H Activation/Nickelation. As already mentioned, our previous experiments[3,4] have shown that the addition of Cs_2CO_3 to the reaction mixture of Ni(Naph)(OPiv)(dcype) (**1B**) and benzoxazole facilitates the stoichiometric reaction and increases its yield from 32% (in no base case) to 67% (for the Cs_2CO_3 case) (Scheme 2). Furthermore, the provided kinetics in the present paper (see Figure 3) on the stoichiometric reaction of **1B** with benzoxazole in the presence and absence of bases (see SI for more details) show that the addition of Cs_2CO_3 to the reaction mixture increases rate of the reaction by 3-fold. The above presented computational data are fully consistent with these experimental findings. In addition, the presented computations provided detailed understanding of the factors impacting the reported base effect: it was shown that (1) the addition of base leads to formation of the thermodynamically stable cluster complex **3_Cs_clus** rather than the $PivO^- \rightarrow CsCO_3^-$ ligand exchange, and (2) the coordination of substrate (benzoxazole) to the resultant cluster complex **3_Cs_clus** forms prereaction complex with Cs-heteroatom(azole) interactions that increases the acidity of the activated C−H bond and is predicted to be one of the factors lowering the C−H activation barrier.

In order to provide additional support to the presented mechanistic details of the base effect, we performed computational study of the reaction mechanism of **1B** with benzoxazole in the presence of K_2CO_3. Since all calculated intermediates and transition states of the reaction of **1B** with benzoxazole in the presence of K_2CO_3 are found to be similar to those in the case of Cs_2CO_3, we included them in SI. Importantly, these new calculations provide 28.2 and 32.5 kcal/mol C−H activation/nickelation barriers at the 298.15 and 373.15 K, respectively. These values are smaller than that, 31.0 and 34.7 kcal/mol, respectively, reported for the no base case, but are slightly larger than 27.3 and 31.1 kcal/mol, respectively, found for the Cs_2CO_3 case. In other words, the reaction of **1B** with benzoxazole in the presence of K_2CO_3 should be more efficient than that without any base, but less efficient than that in the presence of Cs_2CO_3. The increase in the calculated C−H activation barrier upon going from the Cs_2CO_3 base case to the K_2CO_3 base case could be attributed to the weaker K−N(azole) interaction compared to the Cs−N(azole) interaction (see SI).

In order to test the computationally predicted trend in the reactivity of the stoichiometric reaction of **1B** with benzoxazole, i.e., no base < K_2CO_3 < Cs_2CO_3, we experimentally studied [under the same experimental conditions as that for the Cs_2CO_3 case] the stoichiometric reaction of Ni(Naph)(OPiv)(dcype) (**1B**) and benzoxazole in the presence of K_2CO_3 (i.e., the $Cs_2CO_3 \rightarrow K_2CO_3$ substitution) as well. Consistent with the presented computational prediction, we found that the addition of K_2CO_3 to the reaction mixture of **1B** and benzoxazole increases the reaction yield (from 32% to 51%) and makes the reaction slightly faster (by 1.1-fold). In other words, while the provided kinetic studies confirm the computationally predicted trend in the reactivity of the stoichiometric reaction of **1B** with benzoxazole, i.e., no base < K_2CO_3 < Cs_2CO_3, in the experimental condition, the base effect is somewhat more pronounced for Cs_2CO_3 than for K_2CO_3.

3.2.2. Effect of C−H Substrate. Above we predicted that the existence of the Cs-heteroatom(azole) interaction in the (**3_Cs_clus**)-(benzoxazole) prereaction complex facilitates the benzoxazole C−H activation by increasing its acidity (or reducing its pK_a value). In fact, the pK_a value was previously shown to be one of the important factors of C−H bond activation by transition-metal systems.[29] However, a question that still requires more investigations: Is the presence of this Cs-heteroatom(azole) interaction and related pK_a values the only factors impacting the C−H activation by **3_Cs_clus**? In order to reveal other factors affecting C−H activation by **3_Cs_clus**, we investigated the reaction of **1B** with 1H-benzo[d]imidazole (**1b**) and quinazoline (**1c**) in the presence of Cs_2CO_3 both computationally (at the M06L/BS1 level of theory) and experimentally.

Our experiments show that although benzoxazole (**1a**) cross-couples with NaphOPiv in quantitative yield under the standard catalytic conditions, neither 1*H*-benzo[*d*]imidazole (**1b**) nor quinazoline (**1c**) react with NaphOPiv under otherwise identical conditions (Figure 11). Close comparison of these substrates shows that the π-electron density in the azole system decreases in the order **1a** > **1b** > **1c**. This electronic feature of the examined azoles may have a large effect on the Cs-heteroatom(azole) interaction in **4_Cs_clus_N** and the following C−H activation transition state **TS1_Cs_clus_N**.

Consistent with this experimental finding, accompanying calculations show a significant increase in the C−H activation barrier upon replacing **1a** by **1b** or **1c**: from 26.7 kcal/mol in **1a** to 40.2 and 48.6 kcal/mol in **1b** and **1c**, respectively (see Figure 11, these values are obtained at the M06L/BS1 level of theory, in

dx.doi.org/10.1021/ja5071174 | J. Am. Chem. Soc. 2014, 136, 14834−14844

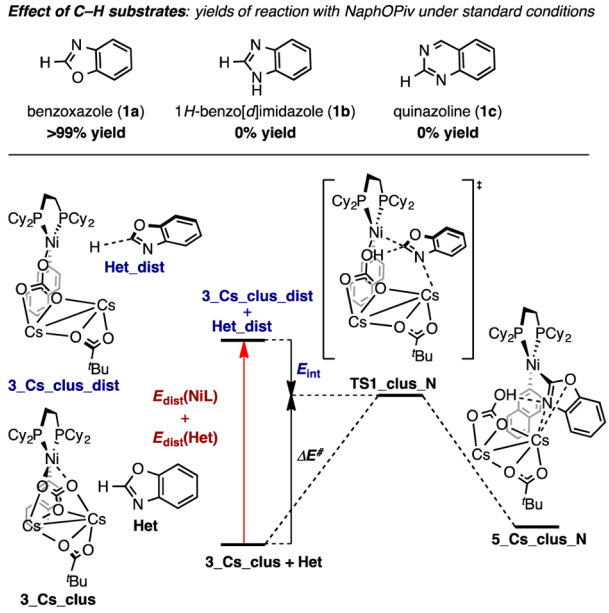

Substrate	$\Delta G^{\ddagger}$	$\Delta E^{\ddagger}$	E_{dist}(NiL)	E_{dist}(Het)	E_{int}
1a	26.6	13.4	25.0	88.1	–99.7
1b	40.2	23.5	28.2	78.4	–83.2
1c	48.6	32.9	23.7	68.4	–59.2

Figure 11. Schematic presentation (benzoxazole is chosen as an example) of the distortion/interaction analysis for the lowest CMD transition states. Here $\Delta G^{\ddagger}$ and $\Delta E^{\ddagger}$ are the Gibbs free and electronic energy barriers, respectively, calculated at the M06L/BS1 level of theory in 1,4-dioxane.

1,4-dioxane, and at 298.15 K temperature). In other words, reaction of **1B** with 1*H*-benzo[*d*]imidazole (**1b**) and quinazoline (**1c**) cannot proceed even in the presence of Cs_2CO_3.

In order to cast light on the possible reasons of the observed and calculated trend in reactivity of **1a**, **1b**, and **1c** by **3_Cs_clus**, i.e., **1a** ≫ **1b** > **1c**, we performed distortion/interaction analysis.[5a,24,30] As seen in Figure 11, the negative value of total interaction energy E_{int} is 16.5 and 40.5 kcal/mol smaller for **1b** and **1c**, respectively, relative to **1a**. Since E_{int} is combination of the [PivOCs·$CsCO_3$]-Het and Ni-C^5(azole) interaction energies, one should expect that the increasing electron density of azole (via **1a** > **1b** > **1c**) defines the Ni-C^5(azole) covalent interaction, which is also manifested in the calculated Ni–C^5 bond distance in corresponding C–H activation transition states (see SI).

The gain in total interaction energy E_{int} via **1a** > **1b** > **1c** is partly offset by total distortion energy E_{dist} [i.e., E_{dist}(NiL) + E_{dist}(Het)] that associates with distortion of the geometry of catalyst and substrate from their "free" (i.e., separate) states to the corresponding moieties in transition states. As could be expected, the substrate distortion energy, E_{dist}(Het), is larger than that, E_{dist}(NiL), for the catalyst. The calculated total distortion energy E_{dist} is 6.5 and 22.0 kcal/mol smaller for **1b** and **1c**, respectively, than for **1a**. Thus, the reduction in total distortion energy E_{dist} only partly compensates the increase of total interaction energy E_{int} in order of **1a** > **1b** > **1c**.

In other words, the calculated large C–H activation barriers (by 13.6 and 22.0 kcal/mol, respectively, relative to benzoxazole **1a**) for the reaction of 1*H*-benzo[*d*]imidazole (**1b**) and quinazoline (**1c**) with **3_Cs_clus** are partly the result of weaker interactions of **1b** and **1c** with the rest of the cluster complex **3_Cs_clus** at the corresponding transition states (see SI). This effect can be attributed to the decrease of π-electron density in these azoles. Thus, the more π-electron-rich azole has the smaller C–H activation barrier by **3_Cs_clus**. Previously, similar conclusion was made by Gorelsky and co-workers for the Pd-catalyzed arene C–H activation reaction.[29]

4. CONCLUSIONS

From the above presented joint computational and experimental studies of the Ni(cod)(dcype)-catalyzed C–H/C–O biaryl coupling, we may draw the following conclusions:

(1) The C–O oxidative addition of NaphOPiv to Ni(cod)(dcype) proceeds via the five-center C(aryl)–O bond activation transition state and leads to the Ni(Naph)(OPiv)(dcype) (**1B**) intermediate. This finding is in excellent agreement with our previous experiments.[4] Furthermore, the C–O oxidative addition is found to be independent from the absence or presence of base as well as the nature of carbonates (i.e., Cs_2CO_3 and K_2CO_3).

(2) In the absence of Cs_2CO_3 base, the C–H activation/nickelation by **1B**, proceeds via the rate-determining 34.7 kcal/mol CMD energy barrier.

(3) Addition of Cs_2CO_3 base to the reaction mixture of **1B** and azole, at first, forms the stable cluster complex Ni(dcype)(Naph)[PivOCs·$CsCO_3$], **3_Cs_clus**, rather than undergoing the $PivO^- \rightarrow CsCO_3^-$ ligand exchange. Coordination of the azole to the resulting **3_Cs_clus** cluster complex leads to an intermediate with a weak Cs-heteroatom(azole) bond, the existence of which increases the acidity of the activated C–H bond and consequently reduces the C–H activation barrier to 31.1 kcal/mol relative to the no base case. This computational conclusion is consistent with our previous[4] and current experiments showing the addition of Cs_2CO_3 to the reaction mixture of **1B** and benzoxazole increases yield of the C–H/C–O biaryl coupling from 32% to 67% and makes the reaction faster by 3-fold.

(4) The emerging mechanistic details of the stoichiometric reaction of **1B** and substrate in the presence of Cs_2CO_3 were endorsed further by studying the reactions of **1B** and benzoxazole in the presence of K_2CO_3 (i.e., $Cs_2CO_3 \rightarrow K_2CO_3$ replacement) and **1B** and benzimidazoles (O → N change) and quinazoline in the presence of Cs_2CO_3. The calculations have shown the increase the reactivity of the stoichiometric reaction of **1B** with benzoxazole via [no base] < K_2CO_3 < Cs_2CO_3 and the C–H activation barrier by 15–20 kcal/mol upon changing the substrate from benzoxazole (**1a**) to 1*H*-benzo[*d*]imidazole (**1b**) or quinazoline (**1c**).

(5) The experiments validated these computational predictions by showing the same trend, i.e., [no base] < K_2CO_3 < Cs_2CO_3, in the reactivity of the stoichiometric reaction of **1B** with benzoxazole, and no coupling reaction between **1B** and either 1*H*-benzo[*d*]imidazole (**1b**) or quinazoline (**1c**) in the presence of Cs_2CO_3.

Based on these findings we proposed a modified catalytic cycle for the Ni(cod)(dcype)-catalyzed C–H/C–O biaryl coupling of benzoxazole and NaphOPiv.

dx.doi.org/10.1021/ja5071174 | J. Am. Chem. Soc. 2014, 136, 14834–14844

■ ASSOCIATED CONTENT

Supporting Information

Cartesian coordinates (*x,y,z*) and energies of all reported structures; Experimental procedure and details; Experimental and computed structures of the Ni(dcype)$(CO)_2$ and oxidative addition product Ni(Naph)(OPiv)(dcype), **1B**; Energies and structures of the pre-reaction complex Ni(dcype(NaphPivO); Potential energy profile of the C−O oxidative addition of naphthalen-2-yl pivalate in various prereaction complexes; Aggregated states of the Cs_2CO_3 and K_2CO_3 molecules; Full potential energy profile of the C−H activation/nickelation in absence of base; Full potential energy profile of the C−H bond activation via *arm-off* mechanism; The C−H activation/nickelation in presence of Cs_2CO_3 base; The C−H activation/nickelation in presence of K_2CO_3 base; The C−H substrate effect in the C−H activation/nickelation; and Calculated structures and relative energies of the 1,4-dioxane solvated **3_Cs_clus** and **4_Cs_clus_N** cluster complexes. These materials are available free of charge via the Internet at http://pubs.acs.org.

■ AUTHOR INFORMATION

Corresponding Authors

dmusaev@emory.edu

itami@chem.nagoya-u.ac.jp

Notes

The authors declare no competing financial interest.

■ ACKNOWLEDGMENTS

The computational studies of this work were supported by the National Science Foundation under the CCI Center for Selective C−H Functionalization (CHE-1205646). The authors gratefully acknowledge NSF MRI-R2 grant (CHE-0958205) and the use of the resources of the Cherry Emerson Center for Scientific Computation. H.X. acknowledges the financial support from China Scholarship Council (CSC).

■ REFERENCES

(1) For the transition-metal-catalyzed C−H functionalization, see: (a) Zheng, C.; You, S.-L. *RSC Adv.* **2014**, *4*, 6173−6214. (b) Rouquet, G.; Chatani, N. *Angew. Chem., Int. Ed.* **2013**, *52*, 11726−11743. (c) Yamaguchi, J.; Yamaguchi, A. D.; Itami, K. *Angew. Chem., Int. Ed.* **2012**, *51*, 8960−9009. (d) Davies, H. M.; Manning, J. R. *Nature* **2008**, *451*, 417−424. (e) Seregin, I. V.; Gevorgyan, V. *Chem. Soc. Rev.* **2007**, *36*, 1173−1193. (f) Cho, S. H.; Kim, J. Y.; Kwak, J.; Chang, S. *Chem. Soc. Rev.* **2011**, *40*, 5068−5083. (g) Kuhl, N.; Hopkinson, M. N.; Wencel-Delord, J.; Glorius, F. *Angew. Chem., Int. Ed.* **2012**, *51*, 10236−10254. (h) Baudoin, O. *Chem. Soc. Rev.* **2011**, *40*, 4902−4911. (i) Lyons, T. W.; Sanford, M. S. *Chem. Rev.* **2010**, *110*, 1147−1169. (j) Wu, N.; Song, F.; Yan, L.; Li, J.; You, J. *Chem.—Eur. J.* **2014**, *20*, 3408−3414.

(2) (a) Alberico, D.; Scott, M. E.; Lautens, M. *Chem. Rev.* **2007**, *107*, 174−238. (b) Chiusoli, G. P.; Catellani, M.; Costa, M.; Motti, E.; Della Ca', N.; Maestri, G. *Coord. Chem. Rev.* **2010**, *254*, 456−469. (c) Sierra, D.; Bhuvanesh, N.; Reibenspies, J. H.; Gladysz, J. A.; Klahn, A. H. *J. Organomet. Chem.* **2014**, *749*, 416−420. (d) Han, F.-S. *Chem. Soc. Rev.* **2013**, *42*, 5270−5298.

(3) Muto, K.; Yamaguchi, J.; Itami, K. *J. Am. Chem. Soc.* **2012**, *134*, 169−172.

(4) Muto, K.; Yamaguchi, J.; Lei, W.; Itami, K. *J. Am. Chem. Soc.* **2013**, *135*, 16384−16387.

(5) (a) Hong, X.; Liang, Y.; Houk, K. N. *J. Am. Chem. Soc.* **2014**, *136*, 2017−2025. (b) Liu, L.; Zhang, S.; Chen, H.; Lv, Y.; Zhu, J.; Zhao, Y. *Chem.—Asian J.* **2013**, *8*, 2592−2595.

(6) Lu, Q.; Yu, H.; Fu, Y. *J. Am. Chem. Soc.* **2014**, *136*, 8252−8260.

(7) Amaike, K.; Muto, K.; Yamaguchi, J.; Itami, K. *J. Am. Chem. Soc.* **2012**, *134*, 13573−13576.

(8) Frisch, M. J.; Trucks, G. W.; Schlegel, H. B.; Scuseria, G. E.; Robb, M. A.; Cheeseman, J. R.; Scalmani, G.; Barone, V.; Mennucci, B.; Petersson, G. A.; Nakatsuji, H.; Caricato, M.; Li, X.; Hratchian, H. P.; Izmaylov, A. F.; Bloino, J.; Zheng, G.; Sonnenberg, J. L.; Hada, M.; Ehara, M.; Toyota, K.; Fukuda, R.; Hasegawa, J.; Ishida, M.; Nakajima, T.; Honda, Y.; Kitao, O.; Nakai, H.; Vreven, T.; Montgomery, J. A., Jr.; Peralta, J. E.; Ogliaro, F.; Bearpark, M.; Heyd, J. J.; Brothers, E.; Kudin, K. N.; Staroverov, V. N.; Keith, T.; Kobayashi, R.; Normand, J.; Raghavachari, K.; Rendell, A.; Burant, J. C.; Iyengar, S. S.; Tomasi, J.; Cossi, M.; Rega, N.; Millam, J. M.; Klene, M.; Knox, J. E.; Cross, J. B.; Bakken, V.; Adamo, C.; Jaramillo, J.; Gomperts, R.; Stratmann, R. E.; Yazyev, O.; Austin, A. J.; Cammi, R.; Pomelli, C.; Ochterski, J. W.; Martin, R. L.; Morokuma, K.; Zakrzewski, V. G.; Voth, G. A.; Salvador, P.; Dannenberg, J. J.; Dapprich, S.; Daniels, A. D.; Farkas, O.; Foresman, J. B.; Ortiz, J. V.; Cioslowski, J.; Fox, D. J. *Gaussian 09*, Revision D.01; Gaussian, Inc.: Wallingford CT, 2013.

(9) Zhao, Y.; Truhlar, D. G. *J. Chem. Phys.* **2006**, *125*, 194101.

(10) (a) Wadt, W. R.; Hay, P. J. *J. Chem. Phys.* **1985**, *82*, 284−298. (b) Hay, P. J.; Wadt, W. R. *J. Chem. Phys.* **1985**, *82*, 299−310.

(11) (a) Mennucci, B.; Tomasi, J. *J. Chem. Phys.* **1997**, *106*, 3032−3041. (b) Mennucci, B.; Tomasi, J. *J. Chem. Phys.* **1997**, *106*, 5151−5158. (c) Scalmani, G.; Frisch, M. J. *J. Chem. Phys.* **2010**, *132*, 114110.

(12) For M06 method see: (a) Zhao, Y.; Truhlar, D. G. *Theor. Chem. Acc.* **2008**, *120*, 215−241. (b) Zhao, Y.; Truhlar, D. G. *Acc. Chem. Res.* **2008**, *41*, 157−167. (c) Zhao, Y.; Truhlar, D. G. *J. Chem. Theory Comput.* **2009**, *5*, 324−333.

(13) (a) Garcia, J. J.; Brunkan, N. M.; Jones, W. D. *J. Am. Chem. Soc.* **2002**, *124*, 9547−9555. (b) Yoshikai, N.; Matsuda, H.; Nakamura, E. *J. Am. Chem. Soc.* **2008**, *130*, 15258−15259.

(14) (a) Quasdorf, K. W.; Antoft-Finch, A.; Liu, P.; Silberstein, A. L.; Komaromi, A.; Blackburn, T.; Ramgren, S. D.; Houk, K. N.; Snieckus, V.; Garg, N. K. *J. Am. Chem. Soc.* **2011**, *133*, 6352−6363. (b) Li, Z.; Zhang, S.-L.; Fu, Y.; Guo, Q.-Z.; Liu, L. *J. Am. Chem. Soc.* **2009**, *131*, 8815−8823.

(15) (a) Lafrance, M.; Rowley, C. N.; Woo, T. K.; Fagnou, K. *J. Am. Chem. Soc.* **2006**, *128*, 8754−8756. (b) Gorelsky, S. I.; Lapointe, D.; Fagnou, K. *J. Am. Chem. Soc.* **2008**, *130*, 10848−10849.

(16) (a) Birkholz, M.-N.; Freixa, Z.; van Leeuwen, P. W. N. M. *Chem. Soc. Rev.* **2009**, *38*, 1099−1118. (b) Clegg, W.; Eastham, G. R.; Elsegood, M. R. J.; Heaton, B. T.; Iggo, J. A.; Tooze, R. P.; Whyman, R.; Zacchini, S. *Organometallics* **2002**, *21*, 1832−1840.

(17) (a) Ananikov, V. P.; Musaev, D. G.; Morokuma, K. *Inorg. Chem.* **2007**, *34*, 5390−5399. (b) Ananikov, V. P.; Musaev, D. G.; Morokuma, K. *Organometallics* **2005**, *24*, 715−723. (c) Ananikov, V. P.; Musaev, D. G.; Morokuma, K. *J. Am. Chem. Soc.* **2002**, *124*, 2839−2852.

(18) Figg, T. M.; Wasa, M.; Yu, J.-Q.; Musaev, D. G. *J. Am. Chem. Soc.* **2013**, *135*, 14206−14214. (b) Zhang, Q.; Yu, H.-Z.; Fu, Y. *Organometallics* **2013**, *32*, 4165−4173.

(19) Ackermann, L. *Chem. Rev.* **2011**, *111*, 1315−1345.

(20) For representative selected examples, see: (a) Jazzar, R.; Hitce, J.; Renaudat, A.; Sofack-Kreutzer, J.; Baudoin, O. *Chem.—Eur. J.* **2010**, *16*, 2654−2672. (b) Lafrance, M.; Gorelsky, S. I.; Fagnou, K. *J. Am. Chem. Soc.* **2007**, *129*, 14570−14571. (c) Rousseaux, S.; Gorelsky, S. I.; Chung, B. K. W.; Fagnou, K. *J. Am. Chem. Soc.* **2010**, *132*, 10692−10705. (d) Dyker, G. *Angew. Chem., Int. Ed. Engl.* **1992**, *31*, 1023−1025. (e) Dyker, G. *J. Org. Chem.* **1993**, *58*, 6426−6428. (f) Barder, T. E.; Walker, S. D.; Martinelli, J. R.; Buchwald, S. L. *J. Am. Chem. Soc.* **2005**, *127*, 4685−4696. (g) Zhao, J.; Campo, M.; Larock, R. *Angew. Chem., Int. Ed.* **2005**, *44*, 1873−1875. (h) Dong, C.-G.; Hu, Q.-S. *Angew. Chem., Int. Ed.* **2006**, *45*, 2289−2292. (i) Ren, H.; Li, Z.; Knochel, P. *Chem.—Asian J.* **2007**, *2*, 416−433. (j) Niwa, T.; Yorimitsu, H.; Oshima, K. *Org. Lett.* **2007**, *9*, 2373−2375. (k) Dong, C.-G.; Hu, Q.-S. *Tetrahedron* **2008**, *64*, 2537−2552. (l) Mousseau, J. J.; Lariv_ee, A.; Charette, A. B. *Org. Lett.* **2008**, *10*, 1641−1643. (m) Salcedo, A.; Neuville, L.; Zhu, J. *J. Org. Chem.* **2008**, *73*, 3600−3603. (n) Niwa, T.; Yorimitsu, H.; Oshima, K. *Org. Lett.* **2008**, *10*,

4689−4691. (o) Kim, H. S.; Gowrisankar, S.; Kim, S. H.; Kim, J. N. *Tetrahedron Lett.* **2008**, *49*, 3858−3861. (p) Huang, Q.; Larock, R. C. *Tetrahedron Lett.* **2009**, *50*, 7235−7238. (q) Wasa, M.; Engle, K. M.; Yu, J.-Q. *J. Am. Chem. Soc.* **2009**, *131*, 9886−9887. (r) Kim, K. H.; Lee, H. S.; Kim, S. H.; Kim, S. H.; Kim, J. N. *Chem.—Eur. J.* **2010**, *16*, 2375−2380 and references cited therein.

(21) Lian, B.; Zhang, L.; Chass, G. A.; Fang, D.-C. *J. Org. Chem.* **2013**, *78*, 8376−8385.

(22) (a) Mateos, C.; Mendiola, J.; Carpintero, M.; Minguez, J. M. *Org. Lett.* **2010**, *12*, 4924−4927. (b) Sun, H.-Y.; Gorelsky, S. I.; Stuart, D. R.; Campeau, L.-C.; Fagnou, K. *J. Org. Chem.* **2010**, *75*, 8180−8189.

(23) See these articles and references therein: (a) Garcia-Cuadrado, D.; Braga, A. A. C.; Maseras, F.; Echavarren, A. M. *J. Am. Chem. Soc.* **2006**, *128*, 1066−1067. (b) Garcia-Cuadrado, D.; de Mendoza, P.; Braga, A. A. C.; Maseras, F.; Echavarren, A. M. *J. Am. Chem. Soc.* **2007**, *129*, 6880−6886. (c) Kefalidis, C. E.; Baudoin, O.; Clot, E. *Dalton Trans.* **2010**, *39*, 10528−10535.

(24) Mahler, J.; Persson, I. *Inorg. Chem.* **2012**, *51*, 425−438.

(25) Robinson, S.; Davies, E. S.; Lewis, W.; Blake, A. J.; Liddle, S. T. *Dalton Trans.* **2014**, *43*, 4351−4360.

(26) Edelmann, F. T.; Pauer, F.; Wedler, M.; Stalke, D. *Inorg. Chem.* **1992**, *31*, 4143−4146.

(27) Gorelsky, S. I. *Organometallics* **2012**, *31*, 794−797.

(28) From the complexes **5_Cs_clus_O** and **5_Cs_clus_N** the reaction may proceed via either: (a) the [PivOCs·$CsHCO_3$] dissociation and then C−C reductive elimination or (b) the C−C reductive elimination and then [PivOCs·$CsHCO_3$] dissociation. Calculations show that the [PivOCs·$CsHCO_3$] dissociation from intermediates **5_Cs_clus_O** and **5_Cs_clus_N** is ΔG = 9.0 and 7.6 kcal/mol endergonic and the subsequent reductive elimination requires $\Delta G^{\ddagger}$ = 9.0 kcal/mol energy barrier. On the other hand, the direct C−C reductive elimination from **5_Cs_clus_O** and **5_Cs_clus_N** requires $\Delta G^{\ddagger}$ = 11.5 and 9.9 kcal/mol energy barrier at the transition states **TS2_Cs_clus_O** and **TS2_Cs_clus_N**, respectively (see SI). Therefore, it is expected that the C−C coupling will directly occur from the intermediates **5_Cs_clus_O** and **5_Cs_clus_N** via corresponding transition states **TS2_Cs_clus_O** and **TS2_Cs_clus_N** and will lead to the product complexes **6_Cs_clus_O** and **6_Cs_clus_N**, respectively.

(29) For example, see: Shen, K.; Fu, Y.; Li, J.-N.; Liu, L.; Guo, Q.-X. *Tetrahedron* **2007**, *63*, 1568−1576.

(30) (a) Ref 15b. (b) Gorelsky, S. I.; Lapointe, D.; Fagnou, K. *J. Org. Chem.* **2011**, *77*, 658−668.